Nonlinear dynamics of rapidly driven systems

Afshin Besharat* and Alexander A. Penin†
Department of Physics, University of Alberta, Edmonton, Alberta T6G 2J1, Canada

(Received 30 July 2026; accepted 21 October 2026; published 10 November 2026)

We consider systems characterized by the presence of a rapidly oscillating force. A general method is presented for the construction of the effective action governing the large-scale nonlinear dynamics of such systems order by order in inverse powers of the oscillation frequency ω. The explicit expression for the effective Lagrangian is derived up to $\mathcal{O}(1/\omega^6)$ next-to-next-to-leading approximation in the strong-drive regime. The general structure of the high-frequency expansion reveals a broad class of nonlinear systems whose transition curves are identical to those of the linear Mathieu equation, which enables a fully nonperturbative stability analysis in the case of strong driving and nonlinearity. The method is generalized to velocity-dependent forces and configuration space with curvature, characteristic to systems with constraints. Several applications are discussed in detail, including the dynamical magnetic trapping of electric charges.

DOI: 10.1103/46tw-51sh

I. INTRODUCTION

Since the classical work [1] the dynamics of particles in a rapidly oscillating field has been studied in a wide range of problems from dynamical chaos [2,3] to quantum computing [4,5] and Floquet engineering of quantum materials [6,7] with the renowned application in the design of the ion traps [8] as well as the neutral atom traps [9,10]. Theoretical description of this class of systems is based on the concept of averaging, when the effect of the oscillating field is smeared out and the long-time evolution is governed by the resulting effective interaction naturally obtained as a series in the ratio of the oscillation period to a characteristic timescale of the averaged system. However, most of the applications so far deal with the leading-order approximation in the high-frequency limit. The role of the high-order and nonlinear effects remains a fundamental open question in the theory of dynamical stabilization. Given the long history and the importance of the problem, surprisingly little has been known about the high-order behavior of the generic nonlinear three-dimensional systems, despite numerous studies performed within different frameworks (see Refs. [11–20] and references therein). The main challenge of the perturbative analysis is in finding an algorithm of a systematic *high-frequency expansion* for the time-averaged effective action, which renders high-order calculations feasible. Such an algorithm has been recently introduced in a letter [21], where the explicit next-to-leading result has been obtained for the three-dimensional systems, and the analysis has been forced through the next-to-next-to-leading order in the case of one dimension. A remarkable finding in Ref. [21] is that beyond the leading order the systems reveal highly nontrivial nonlinear behavior—the trajectories of the particles in the rapidly oscillating fields coincide with the geodesics in a Riemann space with the curvature determined by the spatial distribution of the oscillating field amplitude, i.e., the systems emulate post-Newtonian general relativity.

In this paper we give a detailed account of the method [21], present the calculation of the effective action in any number of spatial dimensions up to the next-to-next-to-leading order, and describe the generalization of the method to the velocity-dependent forces and to the configuration space with curvature, naturally appearing in the mechanical systems with constraints. A general criterion is formulated determining when the stability analysis of a rapidly driven nonlinear system can be reduced to that of the linear Mathieu equation to all orders of the high-frequency expansion, thereby extending the results beyond the perturbation theory. We present explicit solutions for a number of mechanical systems including the classical problem of Kapitza pendulum. Finally, the method is applied to the charged particle dynamics in the inhomogeneous rapidly oscillating magnetic field, which sets up the foundation for the new type of dynamical magnetic traps [22].

II. GENERAL FORMALISM

Our starting point is the classical equation of motion for a particle of mass m subjected to a static force $-\boldsymbol{G}$ and a periodic force $-\boldsymbol{F}\cos\omega t$,

$$m\ddot{\boldsymbol{R}} + \boldsymbol{G}(\boldsymbol{R}) + \boldsymbol{F}(\boldsymbol{R})\cos\omega t = 0, \tag{1}$$

where the dot stands for the time derivative d/dt and the bold fonts indicate d-dimensional vectors for any d. The periodic drive is limited to a single harmonic for the clarity of the presentation but the inclusion of higher harmonics is rather straightforward. We do not specify the nature of the external fields to keep the discussion general and consider the limit of fast oscillation. Let us quantify this condition as it plays a crucial role for the determination of the expansion parameter and the power counting rules. For a system of a characteristic size L a typical velocity acquired by the particle under the action of the time-independent force is $v \sim (GL/m)^{1/2}$.

*Contact author: abeshara@ualberta.ca
†Contact author: penin@ualberta.ca

 ©2026 American Physical Society

One can define a "reference" velocity $c = L\omega$ and the oscillations are considered fast when $v/c \ll 1$. Our approach relies on the effective theory concept to separate the "slow" large-scale dynamics characterized by the velocity v from the "fast" small-scale dynamics characterized by the velocity c and manifested through the power corrections in the scale ratio to the effective action. It is convenient to introduce the dimensionless variables $\omega t \to t$, $R/L \to R$ so that the equation of motion becomes

$$\ddot{\boldsymbol{R}} + \boldsymbol{g}(\boldsymbol{R}) + \boldsymbol{f}(\boldsymbol{R})\cos t = 0 \tag{2}$$

with $\boldsymbol{g} = \boldsymbol{G}/(Lm\omega^2)$ and $\boldsymbol{f} = \boldsymbol{F}/(Lm\omega^2)$. Note that in the rescaled variables $c = 1$ and the expansion parameter is v. While $\boldsymbol{g} = O(v^2)$ by definition, the scaling of the oscillating term needs to be determined. The leading contribution of the oscillating field to the effective action is quadratic in its amplitude and we are interested in the physical systems where the large-scale dynamics is essentially determined by the effect of the periodic drive, which should be comparable to the one of the static field. This requires $\boldsymbol{f} = O(v)$, i.e., with the rest of the parameters fixed, the amplitude $\boldsymbol{F}$ of the oscillating field should scale linearly with its frequency. This does not necessarily mean the actual dependence of the amplitude on the frequency but rather determines the relevant range for the oscillating field amplitude at a given ω. This corresponds to the "strong-drive" scaling relevant for the study of the dynamical stabilization. The "fixed-drive" regime, where the amplitude $\boldsymbol{F}$ remains constant in the high-frequency limit, implies $\boldsymbol{f} = O(v^2)$ and can be obtained from the strong-drive result by dropping the higher powers of $\boldsymbol{f}$ field in the effective action at a given order of the expansion.

A number of methods have been developed to disentangle the slow and fast dynamics in perturbation theory (see Refs. [23–28] for a review). They share the principal idea of introducing independent variables for the fast and slow evolution with subsequent averaging over the fast one. Its particular realization, however, is crucial to get an efficient tool for the high-order analysis. A natural choice of the slow variable is the path along the smeared trajectory [21]. In this case the solution of Eq. (2) can be formally written as

$$\begin{aligned} \boldsymbol{R} &= \boldsymbol{r} + \delta\boldsymbol{R}, \\ \delta\boldsymbol{R} &= \sum_{n=1}^{\infty} [\boldsymbol{c}_n(\boldsymbol{r})\cos(nt) + \boldsymbol{s}_n(\boldsymbol{r})\sin(nt)], \end{aligned} \tag{3}$$

where the vector $\boldsymbol{r}(t)$ describes the smeared slow motion. Then the total time derivative splits into the slow and fast components as follows:

$$\frac{d}{dt} = \boldsymbol{v}\boldsymbol{\partial} + \partial_t, \tag{4}$$

where $\boldsymbol{\partial} = \partial/\partial\boldsymbol{r}$.[1] Strictly speaking our choice of the slow variable is well defined only for $\boldsymbol{v} \neq 0$. The resulting effective Lagrangian, however, is regular in the limit of vanishing velocity and can be continued to $\boldsymbol{v} = 0$. The slow variation of the $\boldsymbol{r}$ variable is manifested by the requirement that its time derivative $\boldsymbol{v} = \dot{\boldsymbol{r}}$ scales as $\mathcal{O}(v)$ and is a function of $\boldsymbol{r}$ only.[2] Thus the average acceleration $\boldsymbol{a} \equiv \ddot{\boldsymbol{r}} = v_i\partial_i\boldsymbol{v}$ is $\mathcal{O}(v^2)$.[3] By substituting Eqs. (3) and (4) into Eq. (2), after the expansion in v and in the Fourier harmonics one gets the algebraic equations on the harmonic coefficients $\boldsymbol{c}_n$, $\boldsymbol{s}_n$ and the differential equation which determines the time evolution of $\boldsymbol{r}$ order-by-order in the high-frequency expansion. The resulting equation on $\boldsymbol{r}$ is of the form $\boldsymbol{a} + \boldsymbol{\mathcal{F}}_{\rm eff} = 0$ and can be understood as the effective theory equation of motion which governs the slow large-scale evolution of the system under the action of the effective force $-\boldsymbol{\mathcal{F}}_{\rm eff}(\boldsymbol{r}, \boldsymbol{v})$.[4] The resulting function $\boldsymbol{r}(t)$ determines the solution of Eq. (2) through Eq. (3). This approach is reminiscent of the renowned Krylov-Bogoliubov asymptotic method [23,24] which has been originally developed for the nonlinear oscillation theory. There are two main distinction, though: (i) The slow evolution is not limited to the fast-oscillation amplitude variation, and hence Eq. (3) accommodates the zero harmonic, and (ii) the fast modes are determined by the external force, and hence the corrections to the fast-oscillation frequency are absent.

In practice the high-frequency expansion within this framework is realized through the following steps.

(1) We define the series

$$\begin{aligned} \boldsymbol{v} &= \sum_{m=1}^{\infty} \boldsymbol{v}^{(m)}(\boldsymbol{r}), \quad \boldsymbol{a} = \sum_{m=2}^{\infty} \boldsymbol{a}^{(m)}(\boldsymbol{r}), \\ \boldsymbol{c}_n &= \sum_{m=1}^{\infty} \boldsymbol{c}_n^{(m)}(\boldsymbol{r}), \quad \boldsymbol{s}_n = \sum_{m=1}^{\infty} \boldsymbol{s}_n^{(m)}(\boldsymbol{r}), \end{aligned} \tag{5}$$

where the mth term of each series uniformly scales as $\mathcal{O}(v^m)$. Note that the series coefficients of the acceleration and velocity are related as follows:

$$\boldsymbol{a}^{(m)} = \sum_{l=1}^{m-1} v_i^{(l)}\partial_i\boldsymbol{v}^{(m-l)}, \tag{6}$$

and the contribution of the higher harmonics is suppressed: $\boldsymbol{c}_n^{(m)}, \boldsymbol{s}_n^{(m)} = 0$ for $m < n$.

(2) Equations (3), (4), and (5) are substituted into Eq. (2) where the functions $\boldsymbol{g}$ and $\boldsymbol{f}$ are expanded in the series

$$\begin{aligned} \boldsymbol{g}(\boldsymbol{R}) &= \boldsymbol{g}(\boldsymbol{r}) + \sum_{n=1}^{\infty} \frac{1}{n!}(\delta R_{i_n}\cdots\delta R_{i_1})\partial_{i_n}\cdots\partial_{i_1}\boldsymbol{g}(\boldsymbol{r}), \\ \boldsymbol{f}(\boldsymbol{R}) &= \boldsymbol{f}(\boldsymbol{r}) + \sum_{n=1}^{\infty} \frac{1}{n!}(\delta R_{i_n}\cdots\delta R_{i_1})\partial_{i_n}\cdots\partial_{i_1}\boldsymbol{f}(\boldsymbol{r}). \end{aligned} \tag{7}$$

[1]Throughout the paper for every term with a pair of the boldface d-dimensional vectors their scalar product is implied.

[2]Here v is the dimensionless ratio of the parameters of the system defined above. The function $\boldsymbol{v}(\boldsymbol{r})$ describes the time dependence of the velocity on a smeared trajectory $\boldsymbol{r}(t)$ and does not impose any constraint on the independent dynamical variables in the effective theory.

[3]The summation over the repeating indices is implied throughout the paper and $\partial_i \equiv \partial/\partial r_i$.

[4]The negative sign is introduced for convenience and we will refer to $\boldsymbol{\mathcal{F}}_{\rm eff}$ as the effective force in the rest of the paper.

Then Eq. (6) is used to combine the velocity gradient terms into the acceleration at a given order of the expansion.

(3) After the rescaling $\boldsymbol{g} \to \varepsilon^2 \boldsymbol{g}$, $\boldsymbol{f} \to \varepsilon \boldsymbol{f}$, $\{\boldsymbol{v}^{(m)}, \boldsymbol{a}^{(m)}, \boldsymbol{c}_n^{(m)}, \boldsymbol{s}_n^{(m)}\} \to \varepsilon^m \{\boldsymbol{v}^{(m)}, \boldsymbol{a}^{(m)}, \boldsymbol{c}_n^{(m)}, \boldsymbol{s}_n^{(m)}\}$, the resulting Eq. (2) is expanded in the power series in ε and in Fourier harmonics. Equating the contribution of each Fourier harmonic to zero in mth order of ε-expansion provides a set of equations for $\boldsymbol{c}_n^{(m)}$, $\boldsymbol{s}_n^{(m)}$, and $\boldsymbol{a}^{(m)}$ in terms of the lower-order coefficients. The equations on the harmonic coefficients $\boldsymbol{c}_n^{(m)}, \boldsymbol{s}_n^{(m)}$ are *algebraic* since their leading contribution is determined by the fast ∂_t part of the time derivative, Eq. (4), acting on $\cos(nt)$ or $\sin(nt)$ functions in Eq. (3). The remaining equation $\boldsymbol{a}^{(m)} + \boldsymbol{\mathcal{F}}_{\text{eff}}^{(m)} = 0$ defines the effective force at $\mathcal{O}(v^m)$.

(4) The mth-order equations may include the functions $\boldsymbol{a}^{(i)}$ with $i < m$, which are eliminated by the lower-order equations of motion. Moreover, the equations in general include the higher-order time derivatives $\dot{\boldsymbol{a}}$, $\ddot{\boldsymbol{a}}$, ..., which in turn are eliminated through the relations $\dot{\boldsymbol{a}} = -v_i \partial_i \boldsymbol{\mathcal{F}}_{\text{eff}}$, etc., so that the effective force is always a function of $\boldsymbol{r}$ and $\boldsymbol{v}$ only.

Let us now present the results of the explicit calculation through the first few orders of the high-frequency expansion. At $\mathcal{O}(v)$ we get

$$\boldsymbol{c}_1^{(1)} = \boldsymbol{f}, \quad \boldsymbol{s}_1^{(1)} = 0, \quad \boldsymbol{\mathcal{F}}_{\text{eff}}^{(1)} = 0. \tag{8}$$

At $\mathcal{O}(v^2)$ the harmonic coefficients read

$$\begin{aligned} &\boldsymbol{c}_1^{(2)} = 0, \quad \boldsymbol{s}_1^{(2)} = -2 v_i^{(1)} \partial_i \boldsymbol{f}, \\ &\boldsymbol{c}_2^{(2)} = \tfrac{1}{8} f_i \partial_i \boldsymbol{f}, \quad \boldsymbol{s}_2^{(2)} = 0, \end{aligned} \tag{9}$$

and the effective force is given by

$$\boldsymbol{\mathcal{F}}_{\text{eff}}^{(2)} = \boldsymbol{g} + \tfrac{1}{2} f_i \partial_i \boldsymbol{f}. \tag{10}$$

Note that Eq. (10) is valid for arbitrary functions $\boldsymbol{g}$ and $\boldsymbol{f}$. If the corresponding potentials exist so that $\boldsymbol{g} = \boldsymbol{\partial} V_g$ and $\boldsymbol{f} = \boldsymbol{\partial} V_f$, then Eq. (10) can be understood as the Euler-Lagrange equation for the effective Lagrangian,

$$\mathcal{L}_{\text{eff}}^{(2)} = \frac{\boldsymbol{v}^2}{2} - V_{\text{eff}}^{(2)}, \quad V_{\text{eff}}^{(2)} = V_g + \frac{\boldsymbol{f}^2}{4}. \tag{11}$$

At $\mathcal{O}(v^3)$ the nonzero harmonic coefficients are

$$\begin{aligned} \boldsymbol{c}_1^{(3)} &= 3 g_i \partial_i \boldsymbol{f} + f_i \partial_i \boldsymbol{g} + \tfrac{3}{8} f_i f_j \partial_i \partial_j \boldsymbol{f} - 3 v_i^{(1)} v_j^{(1)} \partial_i \partial_j \boldsymbol{f} \\ &\quad + \tfrac{25}{16} f_i (\partial_i f_j) \partial_j \boldsymbol{f}, \\ \boldsymbol{s}_1^{(3)} &= -2 v_i^{(2)} \partial_i \boldsymbol{f}, \\ \boldsymbol{s}_2^{(3)} &= -\tfrac{1}{8} v_i^{(1)} f_j \partial_i \partial_j \boldsymbol{f} - \tfrac{3}{8} v_i^{(1)} (\partial_i f_j) \partial_j \boldsymbol{f}, \\ \boldsymbol{c}_3^{(3)} &= \tfrac{1}{72} f_i f_j \partial_i \partial_j \boldsymbol{f} + \tfrac{1}{144} f_i (\partial_i f_j) \partial_j \boldsymbol{f}, \end{aligned} \tag{12}$$

while the effective force vanishes $\boldsymbol{\mathcal{F}}_{\text{eff}}^{(3)} = 0$. The expressions for the $\mathcal{O}(v^4)$ harmonic coefficients become rather lengthy and are given in Appendix A. Starting with this order the effective force is velocity dependent,

$$\begin{aligned} \boldsymbol{\mathcal{F}}_{\text{eff}}^{(4)} &= -\tfrac{3}{2} v_i^{(1)} v_j^{(1)} \big(\partial_i \partial_j f_k\big) \partial_k \boldsymbol{f} + \tfrac{1}{4} f_i f_j \partial_i \partial_j \boldsymbol{g} \\ &\quad + \big[\tfrac{3}{2} g_i (\partial_i f_k) + \tfrac{1}{2} f_i (\partial_i g_k) + \tfrac{25}{32} f_i (\partial_i f_j)(\partial_j f_k) \\ &\quad + \tfrac{3}{16} f_i f_j (\partial_i \partial_j f_k)\big] \partial_k \boldsymbol{f} + \tfrac{1}{32} f_i f_j (\partial_i f_k) \partial_j \partial_k \boldsymbol{f} \\ &\quad + \tfrac{1}{16} f_i f_j f_k \partial_i \partial_j \partial_k \boldsymbol{f}, \end{aligned} \tag{13}$$

and the corresponding Lagrangian reads

$$\mathcal{L}_{\text{eff}}^{(4)} = -\tfrac{3}{4} v_i v_j (\partial_i \boldsymbol{f}) \partial_j \boldsymbol{f} - V_{\text{eff}}^{(4)}, \tag{14}$$

with the effective potential

$$V_{\text{eff}}^{(4)} = \tfrac{1}{4} f_i \boldsymbol{f} \partial_i \boldsymbol{g} + \tfrac{1}{64} f_i f_j (\partial_i \boldsymbol{f}) \partial_j \boldsymbol{f} + \tfrac{1}{16} f_i f_j \boldsymbol{f} \partial_i \partial_j \boldsymbol{f}. \tag{15}$$

The higher-order harmonic coefficients become too cumbersome and we present only the physically relevant results for the effective force. At $\mathcal{O}(v^5)$ it reads

$$\boldsymbol{\mathcal{F}}_{\text{eff}}^{(5)} = -3 v_i^{(1)} v_j^{(2)} (\partial_i \partial_j f_k) \partial_k \boldsymbol{f}, \tag{16}$$

and can be directly obtained from Eqs. (13) and (14) by keeping the higher-order terms in the expansion of the velocity. The $\mathcal{O}(v^6)$ expression for the force is given in Appendix B. The construction of the corresponding effective Lagrangian, however, is more subtle and is described in Appendix C. The equation of motion with the complex dependence of the effective force on the velocity can only be transformed into the Euler-Lagrange form by a velocity-dependent coordinate transformation $\boldsymbol{r} \to \boldsymbol{r}'(\boldsymbol{r}, \boldsymbol{v})$ with

$$\boldsymbol{r}' = \boldsymbol{r} + \tfrac{5}{3} v_i^{(1)} v_j^{(1)} [(\partial_i \partial_j f_k) \boldsymbol{\partial} f_k - (\partial_i \boldsymbol{\partial} f_k) \partial_j f_k]. \tag{17}$$

Note that since the correction term vanishes at zero velocity, the difference between $\boldsymbol{r}$ and $\boldsymbol{r}'$ vanishes for the system at an equilibrium. Adding up all the contributions through $\mathcal{O}(v^6)$ in new variables we obtain the effective Lagrangian in the next-to-next-to-leading order of the high-frequency expansion,

$$\begin{aligned} \mathcal{L}_{\text{eff}} = \frac{v_i' v_j'}{2} \Big\{ & \delta_{ij} - \frac{3}{2} (\partial_i \boldsymbol{f}) \partial_j \boldsymbol{f} + \frac{5}{6} v_k' v_l' [2 (\partial_i \partial_j \partial_k \boldsymbol{f}) \partial_l \boldsymbol{f} \\ & - (\partial_i \partial_j \boldsymbol{f}) \partial_k \partial_l \boldsymbol{f}] + \frac{5}{3} (2 g_k + f_l \partial_l f_k) [(\partial_i \partial_j \boldsymbol{f}) \partial_k \boldsymbol{f} \\ & - (\partial_i \partial_k \boldsymbol{f}) \partial_j \boldsymbol{f}] - 5 g_k (\partial_k \boldsymbol{f}) \partial_i \partial_j \boldsymbol{f} - 5 g_k (\partial_i \boldsymbol{f}) \partial_j \partial_k \boldsymbol{f} \\ & - 5 (\partial_i f_k) (\partial_k \boldsymbol{g}) \partial_j \boldsymbol{f} - 5 (\partial_i f_k) (\partial_j \boldsymbol{g}) \partial_k \boldsymbol{f} - 3 f_k (\partial_j \boldsymbol{f}) \partial_i \partial_k \boldsymbol{g} \\ & - \frac{5}{2} f_k (\partial_k f_l) (\partial_l \boldsymbol{f}) \partial_i \partial_j \boldsymbol{f} - \frac{43}{16} f_k (\partial_k f_l) (\partial_i \boldsymbol{f}) \partial_l \partial_j \boldsymbol{f} \\ & - \frac{11}{4} f_k (\partial_i f_l) (\partial_j \boldsymbol{f}) \partial_k \partial_l \boldsymbol{f} - \frac{183}{64} f_k (\partial_i f_l) (\partial_l \boldsymbol{f}) \partial_j \partial_k \boldsymbol{f} \\ & - \frac{3}{128} f_k f_l (\partial_i \partial_k \boldsymbol{f}) \partial_j \partial_l \boldsymbol{f} - \frac{9}{8} f_k f_l (\partial_i \boldsymbol{f}) \partial_j \partial_k \partial_l \boldsymbol{f} \\ & - \frac{379}{128} (\partial_i f_k) (\partial_k f_l) (\partial_l \boldsymbol{f}) \partial_j \boldsymbol{f} \Big\} - V_{\text{eff}} + \mathcal{O}(v^8), \end{aligned} \tag{18}$$

where $\boldsymbol{v}' = \dot{\boldsymbol{r}}'$, $\boldsymbol{\partial} = \partial / \partial \boldsymbol{r}'$, and the effective potential reads

$$\begin{aligned} V_{\text{eff}} = V_g & + \frac{\boldsymbol{f}^2}{4} + \frac{1}{4} f_i \boldsymbol{f} \partial_i \boldsymbol{g} + \frac{1}{64} f_i f_j (\partial_i \boldsymbol{f}) \partial_j \boldsymbol{f} \\ & + \frac{1}{16} f_i f_j \boldsymbol{f} \partial_i \partial_j \boldsymbol{f} - \frac{5}{4} g_i g_j (\partial_i \boldsymbol{f}) \partial_j \boldsymbol{f} \\ & + \frac{1}{4} f_i f_j (\partial_i \boldsymbol{g}) \partial_j \boldsymbol{g} - \frac{5}{4} g_i f_j (\partial_i \boldsymbol{f}) (\partial_j f_k) \partial_k \boldsymbol{f} \\ & + \frac{1}{256} f_i f_j (\partial_i f_k) (\partial_j \boldsymbol{f}) \partial_k \boldsymbol{g} + \frac{1}{32} f_i f_j (\partial_i f_k) (\partial_k \boldsymbol{f}) \partial_j \boldsymbol{g} \\ & + \frac{3}{16} f_i f_j f_k (\partial_i \partial_j \boldsymbol{f}) \partial_k \boldsymbol{g} + \frac{1}{64} f_i f_j f_k \boldsymbol{f} \partial_i \partial_j \partial_k \boldsymbol{g} \end{aligned}$$

$$+\frac{1}{64}f_i f_j f_k(\partial_i \boldsymbol{f})\partial_j\partial_k \boldsymbol{g}-\frac{1435}{4608}f_i f_j(\partial_i \boldsymbol{f})(\partial_j f_k)(\partial_k f_l)\partial_l \boldsymbol{f}$$
$$+\frac{1}{512}f_i f_j f_k(\partial_i \boldsymbol{f})(\partial_j f_l)\partial_k\partial_l \boldsymbol{f}+\frac{7}{576}f_i f_j f_k(\partial_j f_l)(\partial_l \boldsymbol{f})$$
$$\times\partial_i\partial_k \boldsymbol{f}+\frac{41}{1152}f_i f_j f_k f_l(\partial_i\partial_j \boldsymbol{f})\partial_k\partial_l \boldsymbol{f}+\frac{1}{192}f_i f_j f_k f_l$$
$$\times(\partial_i \boldsymbol{f})\partial_j\partial_k\partial_l \boldsymbol{f}+\frac{1}{384}f_i f_j f_k f_l \boldsymbol{f}\partial_i\partial_j\partial_k\partial_l \boldsymbol{f}. \tag{19}$$

The computer code for Eqs. (18), (19), and (B1) is provided in Ref. [29].

A few comments are in order. First, due to the time-reversal invariance of Eq. (2) the high-frequency expansion is in even powers of $1/\omega$. Then, to facilitate the practical applications it is instructive to transform the result into the physical units. Through the next-to-leading order the effective Lagrangian becomes

$$\mathcal{L}_{\rm eff}=m\frac{v_i v_j}{2}\left(\delta_{ij}-\frac{3}{2}\frac{(\partial_i \boldsymbol{F})\partial_j \boldsymbol{F}}{m^2\omega^4}\right)-\left(V_g+\frac{1}{4}\frac{\boldsymbol{F}^2}{m\omega^2}\right.$$
$$\left.+\frac{1}{4}\frac{F_i \boldsymbol{F}\partial_i \boldsymbol{G}}{m^2\omega^4}+\frac{1}{64}\frac{F_i F_j(\partial_i \boldsymbol{F})\partial_j \boldsymbol{F}}{m^3\omega^6}+\frac{1}{16}\frac{F_i F_j \boldsymbol{F}\partial_i\partial_j \boldsymbol{F}}{m^3\omega^6}\right). \tag{20}$$

In higher orders the physical units can be restored by introducing an extra $1/(m\omega^2)$ factor per each additional power of the spatial derivative, and an extra $m\omega$ factor per each additional power of velocity, so that $v_i\partial_i \to v_i\partial_i/\omega$. Thus, assuming smooth forces, the expansion parameter for the effective potential in the physical units is given by a dimensionless ratio of the $\boldsymbol{F}$ and $\boldsymbol{G}$ field gradients to $m\omega^2$. Note that our power counting corresponds to the strong-drive regime with $\boldsymbol{F}=\mathcal{O}(\omega)$. In the fixed-drive regime with $\boldsymbol{F}=\mathcal{O}(1)$ the last two terms in Eq. (20) become next-to-next-to-leading and should be omitted.

Finally, we note that the above $\mathcal{O}(v^6)$ result may be important for the high-precision analysis of the parametric resonances in the rapidly driven systems [30] and, in particular, of the instabilities due to the overlapping resonances [31–38]. This, however, is beyond the scope of the present work.

III. DYNAMICAL STABILIZATION IN ONE DIMENSION

The structure of the effective theory greatly simplifies in one-dimensional systems. In particular the correction term in Eq. (17) vanishes and no coordinate transformation is necessary in the derivation of the effective Lagrangian. For a generalized coordinate q and arbitrary functions g and f it takes the following form through $\mathcal{O}(v^6)$:

$$\mathcal{L}_{\rm eff}=\frac{\dot q^2}{2}\left[1-\frac{3}{2}f'^2+\frac{5}{6}\dot q^2(2f'f'''-f''^2)-10f'f''g\right.$$
$$-10f'^2g'-3ff'g''-\frac{379}{128}f'^4-\frac{691}{64}ff'^2f''$$
$$\left.-\frac{3}{128}f^2f''^2-\frac{9}{8}f^2f'f'''\right]-V_{\rm eff}+\mathcal{O}(v^8), \tag{21}$$

where dash denotes the derivative d/dq and the effective potential reads

$$V_{\rm eff}=V_g+\frac{f^2}{4}+\frac{f^2g'}{4}+\frac{f^2f'^2}{64}+\frac{f^3f''}{16}-\frac{5}{4}f'^2g^2+\frac{f^2g'^2}{4}$$
$$-\frac{5}{4}ff'^3g+\frac{9}{256}f^2f'^2g'+\frac{3}{16}f^3f''g'+\frac{f^3f'g''}{64}$$
$$+\frac{f^4g'''}{64}-\frac{1435}{4608}f^2f'^4+\frac{65}{4608}f^3f'^2f''+\frac{41}{1152}f^4f''^2$$
$$+\frac{f^4f'f'''}{192}+\frac{f^5f''''}{384}. \tag{22}$$

Equations (21) and (22) can be obtained from the d-dimensional expressions Eqs. (18) and (19) by dimensional reduction [29] and agree with Ref. [21].

The above result is of a particular interest since many physical systems can be reduced to or decomposed into the one-dimensional problems. The high-order result not only is mandatory for establishing the convergence of the high-frequency expansion and increasing the accuracy of the theoretical predictions but also reveals nontrivial general features of the dynamical stabilization of nonlinear systems. Let us discuss one of them. The dynamical stabilization is a phenomenon when the presence of the rapidly oscillating field changes the stability of the static system. Let us assume that the static system is in equilibrium at $q=0$. Excluding the degenerate cases this implies $g(q)=\delta q+\mathcal{O}(q^2)$ with a constant δ. The rapidly oscillating force generates the effective force which may change the stability of the system when

$$\partial_q \mathcal{F}_{\rm eff}|_{q=\dot q=0}=0. \tag{23}$$

If f depends on a parameter ϵ, then Eq. (23) defines δ as a function of ϵ, i.e., a transition curve in the parameter space of the system. Crossing such a curve results in a bifurcation and qualitative change in the system behavior. For $g(q)=\delta q$, $f(q)=\epsilon q$ the problem is reduced to the linear Mathieu equation, where the transition curves can be obtained, e.g., by the method of harmonic balance (see Ref. [39] for a review) or homotopy analysis [40] beyond the perturbation theory for arbitrary finite values of δ and ϵ. In general, for the nonlinear systems the corresponding transition curves are obviously different. Moreover, the high-order contributions to the effective potential depend on the high-order derivatives of the functions g and f, which makes it more and more sensitive to the nonlinear behavior of the forces near the equilibrium position.

There is, however, one remarkable exception. Let us consider an equilibrium point of the static system at $q=0$, so that $g(q)=\delta q+\mathcal{O}(q^2)$. By construction, for all the terms in the effective potential the total number of the derivatives is less than the total power of the g and f functions by two, cf. Eq. (22). Thus one immediately finds that if $f(0)=0$, i.e., $f(q)=\epsilon q+\mathcal{O}(q^2)$, then the contribution of the nonlinear terms in the expansion of $g(q)$ and $f(q)$ about $q=0$ to Eq. (23) vanishes and the corresponding transition curves coincide with those of the linear Mathieu equation to all orders in the high-frequency expansion. The left-hand side of Eq. (23) for the linear Mathieu equation is known to be an analytic function of δ and ϵ near the origin $\delta=\epsilon=0$ [41], and the corresponding Taylor series has a finite radius of

convergence (the explicit result for the series up to $\mathcal{O}(\epsilon^{28})$ as well as the convergence radius estimate can be found in Ref. [19]). Hence, by analytic continuation the equivalence of the transition curves can be extended beyond the high-frequency expansion to arbitrary values of δ and ϵ. This proves the following nontrivial theorem:

For an arbitrary nonlinear system, if the amplitude of the rapidly oscillating force vanishes at an equilibrium point of the static interaction, the corresponding transition curves coincide with those of the linear Mathieu equation.

We should emphasize that if the above condition is not satisfied, then Eq. (23) for a nonlinear system differs from the one of its linearized approximation near the static equilibrium point starting from the next-to-leading order, i.e., the linearization and time-averaging *do not commute*. An interesting problem in this context is to study how a small deviation of $f(0)$ from zero perturbs the transition curves for nonlinear systems, which, however, is beyond the scope of this paper.

The equivalence of the transition curves extends all the nontrivial features of the Mathieu equation stability chart [39,42] to the above class of the nonlinear systems with arbitrary nonlinearity and driving force amplitude. The class of the system satisfying the above condition is quite broad. In particular, it includes all the one-dimensional systems with vanishing static force $g = 0$ for dynamical equilibrium at the zeros of the amplitude f. The generalization of the analysis to multiple spatial dimensions is more subtle. Indeed, the stability chart of a d-dimensional nonlinear system satisfying the above condition reduces to that of a linear system in the same way. However, already the two-dimensional systems may have a more complex stability chart than the Mathieu equation and should be studied casewise (see the example at the end of Sec. V).

A very illustrative application of this theorem is the Kapitza pendulum. For the vertically oscillating pivot we have $g = \delta\sin(\theta)$, $f = \epsilon\sin(\theta)$, where the dimensionless parameters are $\delta = g/(L\omega^2)$, $\epsilon = (\Delta/L)$. Here θ is the angle measured from the downward position, L is the pendulum length, g is the free fall acceleration, and Δ and ω are the pivot oscillation amplitude and frequency, respectively. Note that at the static unstable equilibrium point $\theta = \pi$ the oscillation amplitude vanishes, so that the system belongs to the class discussed above. For the effective potential we get

$$
\begin{aligned}
V_{\rm eff}^{(2)} &= -\delta\cos(\theta) - \frac{\epsilon^2}{8}\cos(2\theta),\\
V_{\rm eff}^{(4)} &= \frac{1}{16}\delta\epsilon^2\cos(\theta) + \frac{1}{32}\epsilon^4\cos(2\theta)\\
&\quad - \frac{1}{16}\delta\epsilon^2\cos(3\theta) - \frac{5}{512}\epsilon^4\cos(4\theta),\\
V_{\rm eff}^{(6)} &= -\frac{367}{2048}\delta\epsilon^4\cos(\theta) - \frac{1993}{73728}\epsilon^6\cos(2\theta)\\
&\quad + \frac{479}{4096}\delta\epsilon^4\cos(3\theta) + \left(\frac{1}{8}\delta^2\epsilon^2 + \frac{57}{2048}\epsilon^6\right)\cos(4\theta)\\
&\quad + \frac{255}{4096}\delta\epsilon^4\cos(5\theta) + \frac{65}{8192}\epsilon^6\cos(6\theta).
\end{aligned}
\tag{24}
$$

Substituting it into Eq. (23) we get

$$
\delta = \frac{\epsilon^2}{2} - \frac{7}{32}\epsilon^4 + \frac{29}{144}\epsilon^6 + \mathcal{O}(\epsilon^8),
\tag{25}
$$

which coincides with the first transition curve of the Mathieu equation [39]. It describes a pitchfork bifurcation corresponding to the dynamical stabilization of the upward equilibrium position discussed in the original work [1]. The corrections to the effective potential have been analyzed using different methods in Refs. [17,19]. Upon the use of the equation of motion, Eqs. (21) and (24) agree with the next-to-leading effective Lagrangian presented in Ref. [19]. In higher orders the comparison of the results is not straightforward since in Ref. [19] the velocity-dependent terms are eliminated from the equation of motion by using the energy conservation. Hence the resulting effective potential depends on the total energy of the system, while we use the standard definition of the Lagrangian independent of the initial conditions. At the same time, the transition curve derived from the result [19] agrees with Eq. (25) through the next-to-next-to-leading order. The method in Ref. [17] relies on a canonical transformation to decouple the fast modes and construct the effective static Hamiltonian for a rapidly driven system. Our result disagrees with the next-to-leading-order Hamiltonian for the Kapitza pendulum presented in this work.

By contrast, for the horizontally oscillating pivot we have $f = \epsilon\cos(\theta)$ so that for the static stable equilibrium point $\theta = 0$ the fast oscillation amplitude does not vanish. In this case the effective potential reads

$$
\begin{aligned}
V_{\rm eff}^{(2)} &= -\delta\cos(\theta) + \frac{\epsilon^2}{8}\cos(2\theta),\\
V_{\rm eff}^{(4)} &= \frac{3}{16}\delta\epsilon^2\cos(\theta) - \frac{1}{32}\epsilon^4\cos(2\theta)\\
&\quad + \frac{1}{16}\delta\epsilon^2\cos(3\theta) - \frac{5}{512}\epsilon^4\cos(4\theta),\\
V_{\rm eff}^{(6)} &= \frac{73}{2048}\delta\epsilon^4\cos(\theta) + \left(\frac{3}{4}\delta^2\epsilon^2 + \frac{1993}{73728}\epsilon^6\right)\cos(2\theta)\\
&\quad - \frac{1233}{4096}\delta\epsilon^4\cos(3\theta) + \left(-\frac{1}{8}\delta^2\epsilon^2 + \frac{57}{2048}\epsilon^6\right)\cos(4\theta)\\
&\quad + \frac{255}{4096}\delta\epsilon^4\cos(5\theta) - \frac{65}{8192}\epsilon^6\cos(6\theta),
\end{aligned}
\tag{26}
$$

and defines a different transition curve

$$
\delta = \frac{\epsilon^2}{2} + \frac{3}{32}\epsilon^4 + \frac{17}{576}\epsilon^6 + \mathcal{O}(\epsilon^8),
\tag{27}
$$

which describes a pitchfork bifurcation corresponding to the dynamical destabilization of the downward equilibrium with the appearance of two symmetric stable equilibria at a nonzero value of the polar angle.

Despite the similarity, the two above cases are principally different for the stability analysis. For the classical setup with the vertically oscillating pivot from the equivalence of

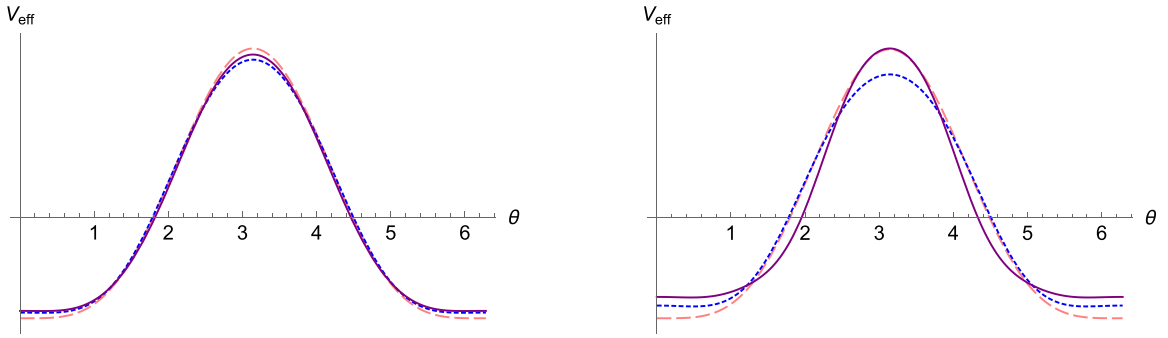


FIG. 1. The convergence of the effective potential for the horizontally driven Kapitza pendulum for the near-critical value of the parameters $\delta = \epsilon^2/2$ for (a) $\epsilon = 1/2$ and (b) $\epsilon = 3/4$. The long-dashed, short-dashed, and solid lines represent the leading, next-to-leading, and next-to-next-to-leading approximations.

the transition curves we conclude that, as for the Mathieu equation, for any δ there are infinitely many narrow stability islands of rapidly decreasing width for the inverted position of the pendulum with infinitely growing ϵ, i.e., the amplitude of the pivot oscillation. The first few of these islands or "tongues" have been observed by a dedicated numerical study in Ref. [43] and indeed agree with the Mathieu equation stability chart. On the contrary, for the horizontally oscillating pivot (in general, for any oscillation direction except strictly vertical) we cannot make any conclusions about the dynamical stabilization beyond the perturbation theory which implies $\epsilon \ll 1$. At the same time we can use the result Eq. (26) to study the actual convergence region of the high-frequency expansion. The effective potential at the near-critical value $\delta = \epsilon^2/2$ in different approximations is plotted in Fig. 1, which clearly indicates breakdown of the perturbation theory for $\epsilon \gtrsim 1/2$. The accuracy of the approximation and the effect of the corrections for the strongly nonlinear oscillations about the dynamically stable equilibrium position close to $\theta = \pi/2$ for different values of the expansion parameter are demonstrated in Fig. 2.

IV. CONFIGURATION SPACE WITH CURVATURE

In Sec. II the particle position in the d-dimensional space was described by the Cartesian coordinates $\boldsymbol{R}$. In many applications, however, the presence of the constraints requires introduction of the generalized coordinates. Let us consider a system with the contravariant generalized coordinates Q^μ in configuration space of arbitrary dimension.[5] Then the kinetic energy can be written as follows $g_{\mu\nu}(Q)\dot{Q}^\mu\dot{Q}^\nu/2$, where $g_{\mu\nu}$ is a symmetric positively defined tensor which can be understood as the metric tensor on the configuration space. If $g_{\mu\nu}$ cannot be globally reduced to the Euclidean form $\delta_{\mu\nu}$ by a coordinate transformation, then the configuration space has nonzero curvature and the effective theory analysis is to be modified. The equations of motion in this case take the form [cf. Eq. (2)]

$$\ddot{Q}^\mu + \Gamma^\mu_{\nu\lambda}(Q)\dot{Q}^\nu\dot{Q}^\lambda + g^\mu(Q) + f^\mu(Q)\cos(t) = 0, \qquad (28)$$

[5]We use the Greek letter indices in this section to distinguish the generalized coordinates from the Cartesian coordinates of Sec. II.

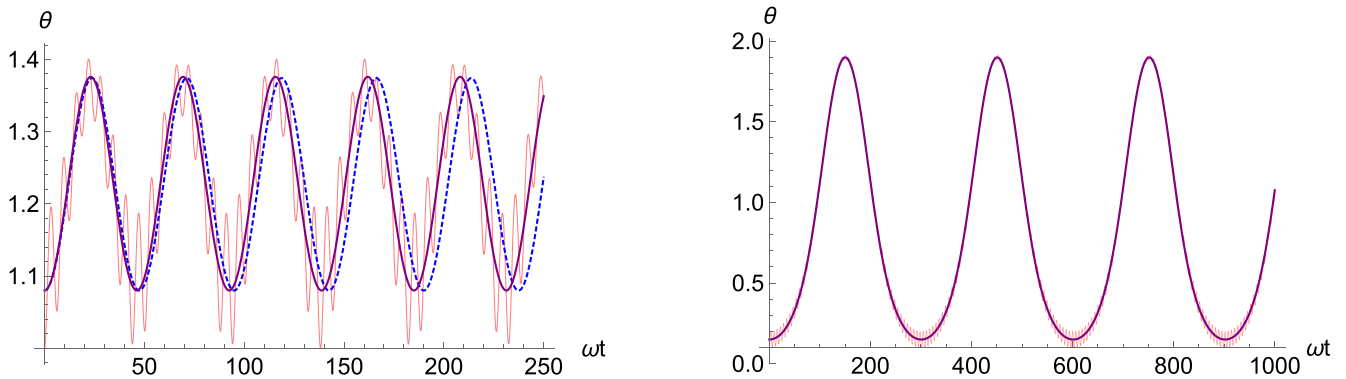
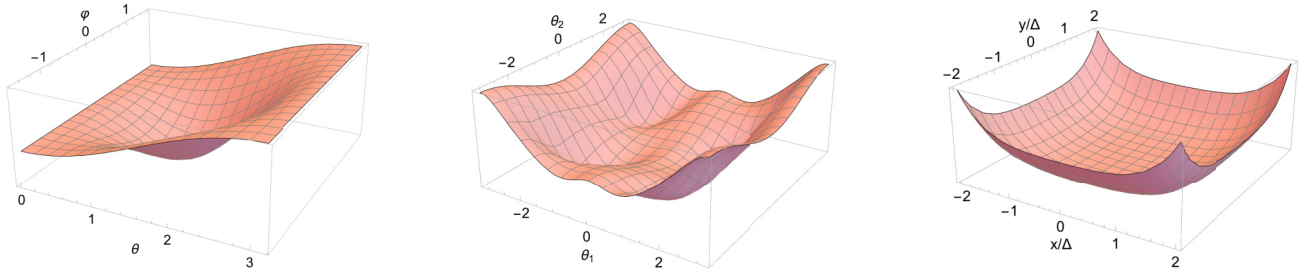


FIG. 2. The solution of the exact equation of motion for the planar pendulum with the horizontally oscillating pivot (thin solid line) *vs* the leading-order (dashed line), and the next-to-leading-order (solid line) effective theory result for (a) $\delta = \epsilon^2/6$, $\epsilon = 1/5$ and (b) $\delta = \epsilon^2/6$, $\epsilon = 1/20$. In the second plot the two effective theory curves are indistinguishable.



(a) (b) (c)

FIG. 3. The effective potential for (a) spherical pendulum with $\delta = \epsilon^2/8$ (the symmetric minimum at $\phi = \pi$ is not shown), (b) planar double pendulum with $\delta = \epsilon^2/6$, and (c) oscillating magnetic field of the Ioffe-Pritchard trap at $z = 0$.

where

$$\Gamma^{\mu}_{\nu\lambda}(Q) = \frac{g^{\mu\kappa}}{2}(\partial_\nu g_{\kappa\lambda} + \partial_\lambda g_{\nu\kappa} - \partial_\kappa g_{\nu\lambda}), \tag{29}$$

are the Christoffel symbols, $g^{\mu\nu} = g^{-1}_{\mu\nu}$, $\partial_\mu = \partial/\partial Q^\mu$, and the contravariant components of a force are obtained from the corresponding potentials in the standard way, e.g.,$f^\mu = g^{\mu\nu} f_\nu$ with $f_\mu = \partial_\mu V_f$.

The high-frequency expansion can be performed through the steps described in Sec. II. We substitute the decomposition

$$Q^\mu = q^\mu + \sum_{n=1}^{\infty} \left[c^\mu_n(q)\cos(nt) + s^\mu_n(q)\sin(nt)\right], \tag{30}$$

and $d/dt = \dot{q}^\mu \partial_\mu + \partial_t$ into Eq. (28) and get the equations for the harmonic coefficients and the time evolution of the slow variables q_μ order by order in inverse frequency. The main difference with the previous analysis is in the presence of the additional metric connection term. At $\mathcal{O}(v)$ we get $c^{\mu(1)}_1 = f^\mu$, and the $\mathcal{O}(v^2)$ effective theory equation of motion becomes

$$\ddot{q}^\mu + \Gamma^\mu_{\nu\lambda}(q)\dot{q}^\nu\dot{q}^\lambda + g^\mu(q) + \tfrac{1}{2} f^\nu(q) D_\nu f^\mu(q) = 0, \tag{31}$$

where $D_\nu f^\mu = \partial_\nu f^\mu + \Gamma^\mu_{\nu\lambda} f^\lambda$ is the covariant derivative. The corresponding effective Lagrangian reads

$$L_{\text{eff}} = \frac{g_{\mu\nu}}{2}\dot{q}^\mu\dot{q}^\nu - V_{\text{eff}}, \quad V_{\text{eff}} = V_g + \frac{1}{4} f^\mu f_\mu. \tag{32}$$

The extension of the analysis to higher orders is straightforward.

As an example let us apply this covariant formalism to two simplest mechanical systems with the curved configuration space. First, we consider a spherical pendulum with the pivot oscillating along the horizontal x axis, where the coordinates are the spherical angles $Q^\mu = (\theta, \phi)$, and the metric tensor is

$$g_{\mu\nu} = \begin{pmatrix} 1 & 0 \\ 0 & \sin^2(\theta) \end{pmatrix}. \tag{33}$$

The exact equations of motion are

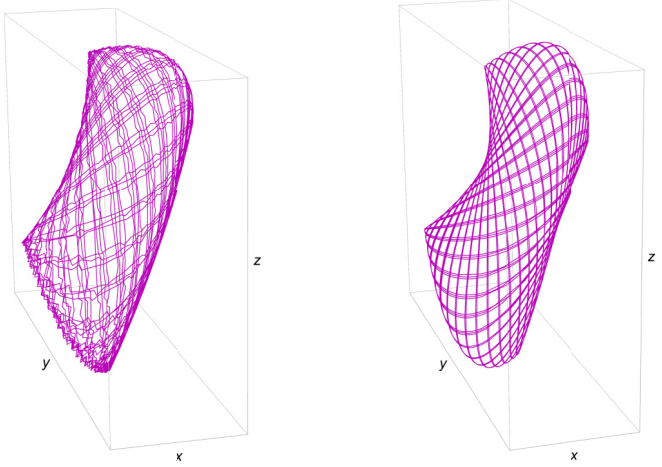
$$\begin{aligned} &\ddot{\theta} - \sin(\theta)\cos(\theta)\dot{\phi}^2 + \delta\sin(\theta) + \epsilon\cos(t)\cos(\phi)\cos(\theta) = 0, \\ &\sin^2(\theta)\ddot{\phi} + 2\cos(\theta)\sin(\theta)\dot{\theta}\dot{\phi} - \epsilon\cos(t)\sin(\phi)\sin(\theta) = 0, \end{aligned} \tag{34}$$

that defines the covariant components of the force $f_\theta = \epsilon\cos(\phi)\cos(\theta)$, $f_\phi = -\epsilon\sin(\phi)\sin(\theta)$. The $\mathcal{O}(v^2)$ effective potential then reads

$$V_{\text{eff}} = -\delta\cos(\theta) + \frac{\epsilon^2}{4}(\cos^2(\theta)\cos^2(\phi) + \sin^2(\phi)), \tag{35}$$

where we used $f^\mu f_\mu = g^{\theta\theta} f^2_\theta + 2g^{\theta\phi} f_\theta f_\phi + g^{\phi\phi} f^2_\phi$ for the covariant square of the vector. The system undergoes a pitchfork bifurcation at $\delta \approx \epsilon^2/2$ with the appearance of two symmetric minima of the effective potential; see Fig. 3(a). The trajectories of the nonlinear oscillations about the dynamical equilibrium position obtained within the full and the effective theory are plotted in Figs. 4(a) and 4(b), respectively.

As the second example we consider a symmetric planar double pendulum with the horizontally oscillating pivot. In this case the coordinates are the polar angles θ_1 and θ_2 of the upper and lower links, respectively, measured from the vertical position. Thus, we have $Q^\mu = (\theta_1, \theta_2)$ and the cor-



(a) (b)

FIG. 4. A trajectory of the spherical pendulum with the horizontally oscillating pivot for $\delta = \epsilon^2/6$, $\epsilon = 1/100$ obtained by solving (a) the exact equations of motion and (b) the effective theory equations of motion.

responding metric tensor can be easily computed

$$g_{\mu\nu} = \begin{pmatrix} 2 & \cos(\theta_1-\theta_2) \\ \cos(\theta_1-\theta_2) & 1 \end{pmatrix}. \tag{36}$$

The exact equations of motion are

$$2\ddot{\theta}_1 + \cos(\theta_1-\theta_2)\ddot{\theta}_2 + \sin(\theta_1-\theta_2)\dot{\theta}_2^{\,2} + 2\delta\sin(\theta_1) + 2\epsilon\cos(t)\cos(\theta_1) = 0,$$

$$\ddot{\theta}_2 + \cos(\theta_1-\theta_2)\ddot{\theta}_1 - \sin(\theta_1-\theta_2)\dot{\theta}_1^{\,2} + \delta\sin(\theta_2) + \epsilon\cos(t)\cos(\theta_2) = 0, \tag{37}$$

where the parameters δ and ϵ are defined as before, with L and m being the length and the mass of each link of the pendulum. From Eq. (37) we find the covariant components $f_{\theta_1} = 2\epsilon\cos(\theta_1)$, $f_{\theta_2} = \epsilon\cos(\theta_2)$, which along with the metric Eq. (36) determine the $\mathcal{O}(v^2)$ effective potential

$$V_{\rm eff} = -\delta(2\cos(\theta_1)+\cos(\theta_2)) + \frac{\epsilon^2}{2}\frac{2\cos^2(\theta_1)+\cos^2(\theta_2)-2\cos(\theta_1-\theta_2)\cos(\theta_1)\cos(\theta_2)}{1+\sin^2(\theta_1-\theta_2)}. \tag{38}$$

The stability chart of this system turns out to be quite interesting. At $\delta \approx \epsilon^2/2$ it undergoes a pitchfork bifurcation similar to the one discussed for the planar and spherical pendula with the dynamical equilibrium configuration corresponding to nonzero θ_1 and θ_2 of the same sign. Then at $\delta \approx \epsilon^2/4$ the second (this time fold) bifurcation takes place and two extra symmetric local minima of the effective potential appear, corresponding to θ_1 and θ_2 of the opposite signs, see Fig. 3(b).

V. DYNAMICAL MAGNETIC CONFINEMENT

In this section we extend the analysis to the systems characterized by the presence of the velocity-dependent and nonpotential forces. The most physically interesting problem in this class is the study of a charged particle motion in the rapidly oscillating magnetic field and related problem of the dynamical magnetic confinement [22].

The equation of motion for a particle of mass m and electric charge e in the rapidly oscillating magnetic field $\boldsymbol{B}(t,\boldsymbol{R}) = \cos(\omega t)\boldsymbol{B}(\boldsymbol{R})$ and the corresponding induced electric field $\boldsymbol{E}(t,\boldsymbol{R}) = \sin(\omega t)\boldsymbol{E}(\boldsymbol{R})$, with $\boldsymbol{\partial}\times\boldsymbol{E}(\boldsymbol{R}) = \omega\boldsymbol{B}(\boldsymbol{R})$, reads[6]

$$\ddot{\boldsymbol{R}} - \frac{e}{m}(\boldsymbol{E}(t,\boldsymbol{R}) + \dot{\boldsymbol{R}}\times\boldsymbol{B}(t,\boldsymbol{R})) = 0. \tag{39}$$

The phase shift between the time-dependent forces, and their nonpotential character require an adjustment of the analysis. Equation (39) is invariant with respect to the time reversal up to the overall phase shift. Hence, the high-frequency expansion is in even powers of $1/\omega$ as in the previous examples. Following the steps described in Sec. II through $\mathcal{O}(1/\omega^4)$ we obtain the harmonic coefficients

$$\boldsymbol{c}_1 = -\frac{ev_j}{m\omega^3}(\boldsymbol{\partial}E_j + \partial_j\boldsymbol{E}),$$
$$\boldsymbol{s}_1 = -\frac{e\boldsymbol{E}}{m\omega^2} + \frac{e}{m\omega^4}v_iv_j(\partial_i\partial_j\boldsymbol{E} + \boldsymbol{\partial}\partial_iE_j + \boldsymbol{\partial}\partial_jE_i), \tag{40}$$

and the effective force

$$\mathcal{F}_{\rm eff} = \frac{e^2}{2m^2\omega^2}E_i\boldsymbol{\partial}E_i + \frac{e^2}{2m^2\omega^4}v_jv_k(-(\partial_j\partial_kE_i)\partial_i\boldsymbol{E} - (\partial_k\partial_iE_j)\boldsymbol{\partial}E_i - (\partial_k\partial_iE_j)\partial_i\boldsymbol{E} + (\partial_iE_j)\boldsymbol{\partial}\partial_iE_k - (\partial_iE_j)\partial_k\partial_i\boldsymbol{E} + (\partial_jE_i)\boldsymbol{\partial}\partial_iE_k - (\partial_jE_i)\partial_k\partial_i\boldsymbol{E}), \tag{41}$$

where we kept the terms quadratic in the electric and magnetic fields and eliminated the latter by the relation $\boldsymbol{B} = \boldsymbol{\partial}\times\boldsymbol{E}/\omega$, so that the result does not explicitly depend on $\boldsymbol{B}$. The corresponding effective Lagrangian reads

$$\mathcal{L}_{\rm eff} = \frac{m}{2}v_iv_j\left[\delta_{ij} - \frac{e^2}{2m^2\omega^4}(\boldsymbol{\partial}E_i\boldsymbol{\partial}E_j + \partial_i\boldsymbol{E}\,\boldsymbol{\partial}E_j + \partial_j\boldsymbol{E}\,\boldsymbol{\partial}E_i)\right] - V_{\rm eff}, \tag{42}$$

with

$$V_{\rm eff} = \frac{e^2}{4m\omega^2}\boldsymbol{E}^2. \tag{43}$$

As an important application of this result, let us consider the magnetic field of the commonly used Ioffe-Pritchard traps [44]

$$\boldsymbol{B}^{(z)} = B\left(\frac{xz}{\Delta^2}, \frac{yz}{\Delta^2}, 1 + \frac{x^2+y^2-2z^2}{2\Delta^2}\right), \tag{44}$$

where B is the value of the homogeneous component of the field [the superscript of $\boldsymbol{B}^{(z)}$ indicates its direction], and an adjustable parameter Δ defines the scale of the field variation determined by the trap geometry. For the oscillating magnetic field with the amplitude Eq. (44) the induced electric field amplitude reads

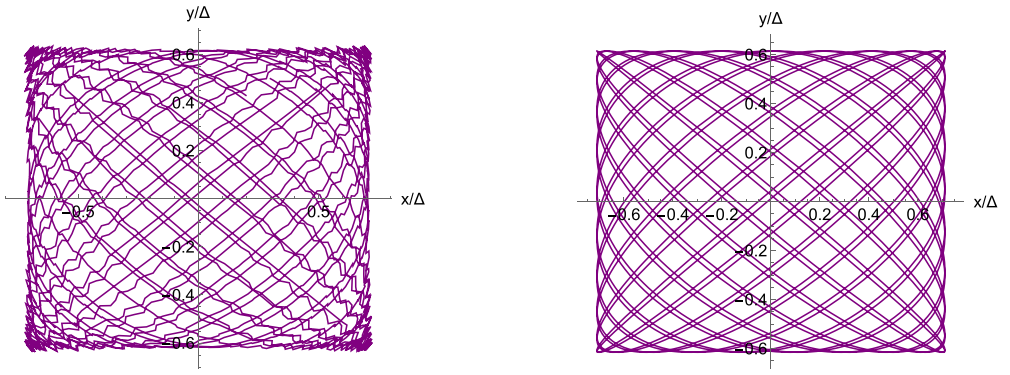
$$\boldsymbol{E} = \frac{\omega B}{2}\left(-y\left(1+\frac{y^2-3z^2}{3\Delta^2}\right), x\left(1+\frac{x^2-3z^2}{3\Delta^2}\right), 0\right). \tag{45}$$

For this field configuration the exact equations of motion are

$$\ddot{x} = \omega_B\left\{-\frac{\omega y}{2}\left(1+\frac{y^2-3z^2}{3\Delta^2}\right)\sin(\omega t) + \left[\dot{y}\left(1+\frac{x^2+y^2-2z^2}{2\Delta^2}\right) - \dot{z}\frac{yz}{\Delta^2}\right]\cos(\omega t)\right\},$$
$$\ddot{y} = \omega_B\left\{\frac{\omega x}{2}\left(1+\frac{x^2-3z^2}{3\Delta^2}\right)\sin(\omega t) + \left[-\dot{x}\left(1+\frac{x^2+y^2-2z^2}{2\Delta^2}\right) + \dot{z}\frac{xz}{\Delta^2}\right]\cos(\omega t)\right\},$$
$$\ddot{z} = \omega_B\left(\dot{x}\frac{yz}{\Delta^2} - \dot{y}\frac{xz}{\Delta^2}\right)\cos(\omega t), \tag{46}$$

where $\omega_B = eB/m$ is the cyclotron frequency associated with the magnetic field oscillation amplitude, and the dimensionless expansion parameter is given by the ratio ω_B^2/ω^2. The

[6] In this section we keep the standard units to facilitate the connection with the experiment.



(a) (b)

FIG. 5. A trajectory of a charged particle in the oscillating magnetic field of the Ioffe-Pritchard trap for $z = 0$, $\omega_B/\omega = 1/20$ obtained by solving (a) the exact equations of motion and (b) the effective theory equations of motion.

effective potential Eq. (43) for the field Eq. (45) takes the form

$$V_{\text{eff}} = \frac{m\omega_B^2}{16}\left[x^2\left(1+\frac{x^2-3z^2}{3\Delta^2}\right)^2 + y^2\left(1+\frac{y^2-3z^2}{3\Delta^2}\right)^2\right]. \tag{47}$$

For the initial values $z = \dot{z} = 0$ the particle motion described by Eq. (46) remains planar and the potential Eq. (47) plotted in Fig. 3(c) provides charge confinement along x and y directions. An example of the full and effective theory trajectories for the motion in the $z = 0$ plane is given in Fig. 5. An unusual rectangular shape of the confining region is due to the anharmonic terms in the potential.

The effective potential Eq. (47) vanishes along the "flat direction" $x^2 = y^2 = 3(z^2 - \Delta^2)$ and, hence, does not provide the confinement in all three dimensions. However, by combining two orthogonal phase-shifted oscillating Ioffe-Pritchard fields we get the rotating magnetic field

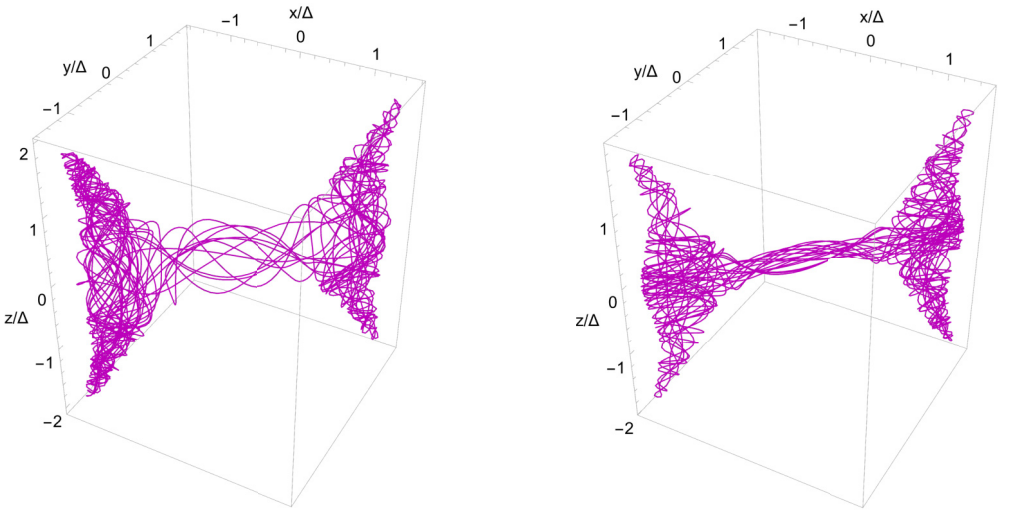
$$\boldsymbol{B}(t,\boldsymbol{r}) = \boldsymbol{B}^{(x)}\cos(\omega t) - \boldsymbol{B}^{(y)}\sin(\omega t), \tag{48}$$

where $\boldsymbol{B}^{(x)}$ and $\boldsymbol{B}^{(y)}$ are obtained by rotating the field Eq. (44) into the x and y directions, respectively

$$\begin{aligned}\boldsymbol{B}^{(x)} &= B\left(1+\frac{y^2+z^2-2x^2}{2\Delta^2}, \frac{yx}{\Delta^2}, \frac{zx}{\Delta^2}\right),\\ \boldsymbol{B}^{(y)} &= B\left(\frac{xy}{\Delta^2}, 1+\frac{z^2+x^2-2y^2}{2\Delta^2}, \frac{zy}{\Delta^2}\right).\end{aligned} \tag{49}$$

It is rather straightforward to derive the effective potential for such a field configuration with the result

$$\begin{aligned}V_{\text{eff}} = \frac{m\omega_B^2}{16}\Bigg[&x^2\left(1+\frac{x^2-3y^2}{3\Delta^2}\right)^2 + y^2\left(1+\frac{y^2-3x^2}{3\Delta^2}\right)^2\\ &+ z^2\left(1+\frac{z^2-3x^2}{3\Delta^2}\right)^2 + z^2\left(1+\frac{z^2-3y^2}{3\Delta^2}\right)^2\Bigg].\end{aligned} \tag{50}$$



(a) (b)

FIG. 6. Same as Fig. 5 but for the three-dimensional magnetic trap and $\omega_B/\omega = 1/50$.

This potential does provide the dynamical magnetic confinement in three dimensions and localizes both positive and negative electric charges in a boxlike region. A typical trajectory in the three-dimensional magnetic trap computed in the full and effective theories is shown in Fig. 6. Though due to the strong nonlinear effects the motion is rather irregular, the effective theory accurately catches the qualitative features of the exact solution. In the limit $\Delta \to \infty$ the magnetic field Eq. (48) becomes homogeneous and the confining potential becomes harmonic, i.e., the effective theory linearizes. Note that though Eq. (46) linearizes in this limit, the resulting system is equivalent to a fourth-order ordinary differential equation with the stability chart different from the Mathieu equation. This case has been discussed in detail in Ref. [22]. Such a rotating locally homogeneous magnetic field is realized in the time-orbiting potential traps for magnetic moment of a neutral particle [45,46], where it plays an auxiliary role to prevent the magnetic moment flip. The inhomogeneous and nonlinear terms, however, could be mandatory for some interesting physical applications. Indeed, an oscillating Ioffe-Pritchard field confines the magnetic moments [22]. Thus, in principle, a trap with the rapidly rotating inhomogeneous magnetic field Eq. (48) can be used to simultaneously confine the positive and negative charges as well as the neutral particles with nonvanishing magnetic moments, which is crucial, e.g., for the antihydrogen production [47,48].

VI. SUMMARY

In this work we have developed a systematic perturbative method for the description of the nonlinear particle dynamics in the presence of rapidly oscillating forces, thereby providing a general solution to the entire class of the problems introduced by the original work [1]. The method is optimized for the calculation of the high-order terms in the high-frequency expansion and offers a powerful tool for the study of dynamical stabilization. It has been applied to a number of real physical systems and verified through the numerical simulations. By analyzing the general all-order structure of the high-frequency expansion we have obtained a nonperturbative description of the stability properties for a broad class of nonlinear systems, including the Kapitza pendulum. Our results can be used in a wide spectrum of applications from the high-precision analysis and design of the particle traps to the Floquet engineering of quantum materials.[7]

ACKNOWLEDGMENTS

The work of A.A.P. was supported in part by NSERC and the Perimeter Institute for Theoretical Physics. The work of A.B. is supported by NSERC.

DATA AVAILABILITY

The data that support the findings of this article are available from the authors upon request.

[7]The analysis of the high-frequency effective theory quantization can be found in Refs. [21,22].

APPENDIX A: $\mathcal{O}(v^4)$ HARMONIC COEFFICIENTS

The nonvanishing harmonic coefficients in the next-to-leading order of the high-frequency expansion read

$$
\begin{aligned}
\boldsymbol{c}_1^{(4)} &= -6v_i^{(1)}v_j^{(1)}\partial_i\partial_j\boldsymbol{f},\\
\boldsymbol{s}_1^{(4)} &= -2v_i^{(3)}\partial_i\boldsymbol{f} - 4v_i^{(1)}(\partial_i f_j)\partial_j\boldsymbol{g} - 12g_i v_j^{(1)}\partial_i\partial_j\boldsymbol{f} - 2f_i v_j^{(1)}\partial_i\partial_j\boldsymbol{g} - 4v_i^{(1)}(\partial_i g_j)\partial_j\boldsymbol{f} - 2v_i^{(1)}f_j(\partial_i f_k)\partial_j\partial_k\boldsymbol{f}\\
&\quad - \tfrac{49}{8}v_i^{(1)}f_j(\partial_j f_k)\partial_i\partial_k\boldsymbol{f} + 4v_i^{(1)}v_j^{(1)}v_k^{(1)}\partial_i\partial_j\partial_k\boldsymbol{f} - \tfrac{3}{4}v_i^{(1)}f_j f_k\partial_i\partial_j\partial_k\boldsymbol{f} - \tfrac{35}{16}v_i^{(1)}f_j(\partial_i\partial_j f_k)\partial_k\boldsymbol{f}\\
&\quad - \tfrac{37}{16}v_i^{(1)}(\partial_i f_j)(\partial_j f_k)\partial_k\boldsymbol{f},\\
\boldsymbol{c}_2^{(4)} &= \tfrac{1}{32}f_i(\partial_i f_j)\partial_j\boldsymbol{g} + \tfrac{3}{32}g_i f_j\partial_i\partial_j\boldsymbol{f} + \tfrac{1}{32}f_i f_j\partial_i\partial_j\boldsymbol{g} + \tfrac{23}{32}g_i(\partial_i f_j)\partial_j\boldsymbol{f} + \tfrac{1}{8}f_i(\partial_i g_j)\partial_j\boldsymbol{f} + \tfrac{1}{16}f_i f_j(\partial_j f_k)\partial_i\partial_k\boldsymbol{f}\\
&\quad - \tfrac{7}{16}v_i^{(1)}v_j^{(1)}(\partial_i f_k)\partial_j\partial_k\boldsymbol{f} + \tfrac{1}{48}f_i f_j f_k\partial_i\partial_j\partial_k\boldsymbol{f} - \tfrac{3}{32}v_i^{(1)}v_j^{(1)}f_k\partial_i\partial_j\partial_k\boldsymbol{f} + \tfrac{7}{144}f_i f_j(\partial_i\partial_j f_k)\partial_k\boldsymbol{f}\\
&\quad - \tfrac{23}{32}v_i^{(1)}v_j^{(1)}(\partial_i\partial_j f_k)\partial_k\boldsymbol{f} + \tfrac{53}{144}f_i(\partial_i f_j)(\partial_j f_k)\partial_k\boldsymbol{f},\\
\boldsymbol{s}_2^{(4)} &= -\tfrac{1}{8}v_i^{(2)}f_j\partial_i\partial_j\boldsymbol{f} - \tfrac{3}{8}v_i^{(2)}(\partial_i f_j)\partial_j\boldsymbol{f},\\
\boldsymbol{s}_3^{(4)} &= -\tfrac{2}{27}v_i^{(1)}f_j(\partial_i f_k)\partial_j\partial_k\boldsymbol{f} - \tfrac{1}{216}v_i^{(1)}f_j(\partial_j f_k)\partial_i\partial_k\boldsymbol{f} - \tfrac{1}{108}v_i^{(1)}f_j f_k\partial_i\partial_j\partial_k\boldsymbol{f} - \tfrac{5}{432}v_i^{(1)}f_j(\partial_i\partial_j f_k)\partial_k\boldsymbol{f}\\
&\quad - \tfrac{11}{432}v_i^{(1)}(\partial_i f_j)(\partial_j f_k)\partial_k\boldsymbol{f},\\
\boldsymbol{c}_4^{(4)} &= \tfrac{1}{2304}f_i f_j(\partial_i\partial_j f_k)\partial_k\boldsymbol{f} + \tfrac{1}{4608}f_i(\partial_i f_j)(\partial_j f_k)\partial_k\boldsymbol{f} + \tfrac{1}{512}f_i f_j(\partial_j f_k)\partial_i\partial_k\boldsymbol{f} + \tfrac{1}{768}f_i f_j f_k\partial_i\partial_j\partial_k\boldsymbol{f}.
\end{aligned}
\tag{A1}
$$

APPENDIX B: $\mathcal{O}(v^6)$ EFFECTIVE FORCE

The effective force in the next-to-next-to-leading order of the high-frequency expansion reads

$$
\begin{aligned}
\mathcal{F}_{\rm eff}^{(6)} &= \tfrac{5}{2}v_i^{(1)}v_j^{(1)}v_k^{(1)}v_l^{(1)}(\partial_i\partial_j\partial_k\partial_l f_m)\partial_m\boldsymbol{f} + \tfrac{3}{2}(\mathcal{F}_{\rm eff}^{(4)})_i(\partial_i f_j)\partial_j\boldsymbol{f} - \tfrac{3}{2}v_i^{(2)}v_j^{(2)}(\partial_i\partial_j f_k)\,\partial_k\boldsymbol{f} - 3\,v_i^{(1)}v_j^{(3)}(\partial_i\partial_j f_k)\partial_k\boldsymbol{f}\\
&\quad + v_i^{(1)}v_j^{(1)}\big[-\tfrac{3}{2}f_k(\partial_i\partial_j\partial_k g_l)\partial_l\boldsymbol{f} - \tfrac{3}{2}f_k(\partial_i\partial_j f_l)\partial_l\partial_k\boldsymbol{g} - 5(\partial_i f_k)(\partial_j\partial_k g_l)\partial_l\boldsymbol{f}
\end{aligned}
$$

$$
\begin{aligned}
&+(\partial_i f_k)(\partial_j f_l)\partial_k\partial_l \boldsymbol{g}-\tfrac{5}{2}(\partial_i\partial_j g_k)(\partial_k f_l)\partial_l \boldsymbol{f}-5(\partial_i\partial_j f_k)(\partial_k g_l)\partial_l \boldsymbol{f}\\
&-10(\partial_i g_k)(\partial_j\partial_k f_l)\partial_l \boldsymbol{f}-15 g_k(\partial_i\partial_j\partial_k f_l)\partial_l \boldsymbol{f}-\tfrac{9}{16} f_k f_l(\partial_i\partial_j\partial_k\partial_l f_m)\partial_m \boldsymbol{f}\\
&-\tfrac{11}{4} f_k(\partial_j f_l)(\partial_i\partial_k\partial_l f_m)\partial_m \boldsymbol{f}-\tfrac{243}{32} f_k(\partial_k f_l)(\partial_j\partial_i\partial_l f_m)\partial_m \boldsymbol{f}-\tfrac{183}{128} f_k(\partial_i\partial_j\partial_k f_l)(\partial_l f_m)\partial_m \boldsymbol{f}\\
&-\tfrac{3}{128} f_k f_l(\partial_l\partial_i\partial_j f_m)\partial_k\partial_m \boldsymbol{f}+\tfrac{1}{4} f_k(\partial_j f_l)(\partial_i f_m)\partial_k\partial_l\partial_m \boldsymbol{f}-\tfrac{9}{16} f_k f_l(\partial_i\partial_j f_m)\partial_k\partial_l\partial_m \boldsymbol{f}\\
&-\tfrac{21}{4} f_k(\partial_i\partial_k f_l)(\partial_j\partial_l f_m)\partial_m \boldsymbol{f}-\tfrac{11}{4} f_k(\partial_j\partial_i f_l)(\partial_k\partial_l f_m)\partial_m \boldsymbol{f}-\tfrac{11}{8}(\partial_i f_k)(\partial_j f_l)(\partial_k\partial_l f_m)\partial_m \boldsymbol{f}\\
&-\tfrac{219}{128}(\partial_i\partial_j f_k)(\partial_k f_l)(\partial_l f_m)\partial_m \boldsymbol{f}-\tfrac{23}{128} f_k(\partial_j\partial_i f_l)(\partial_l f_m)\partial_k\partial_m \boldsymbol{f}-\tfrac{7}{64} f_k(\partial_j f_l)(\partial_i\partial_l f_m)\partial_k\partial_m \boldsymbol{f}\\
&+\tfrac{1}{16} f_k(\partial_j f_l)(\partial_i\partial_k f_m)\partial_l\partial_m \boldsymbol{f}-\tfrac{3}{32} f_k(\partial_k f_l)(\partial_j\partial_i f_m)\partial_l\partial_m \boldsymbol{f}-\tfrac{43}{8}(\partial_i f_k)(\partial_k f_l)(\partial_j\partial_l f_m)\partial_m \boldsymbol{f}\\
&-\tfrac{195}{64}(\partial_i f_k)(\partial_j\partial_k f_l)(\partial_l f_m)\partial_m \boldsymbol{f}+\tfrac{3}{16}(\partial_i f_k)(\partial_j f_l)(\partial_k f_m)\partial_l\partial_m \boldsymbol{f}\big]\\
&+\tfrac{1}{64} f_i f_j f_k f_l\partial_i\partial_j\partial_k\partial_l \boldsymbol{g}+\tfrac{1}{64} f_i f_j f_k(\partial_i f_l)\partial_j\partial_k\partial_l \boldsymbol{g}+\tfrac{1}{16} f_i f_j f_k(\partial_i\partial_j\partial_k g_l)\partial_l \boldsymbol{f}+\tfrac{3}{2} f_i g_j(\partial_j f_k)\partial_i\partial_k \boldsymbol{g}\\
&+\tfrac{1}{2} f_i f_j(\partial_i g_k)\partial_j\partial_k \boldsymbol{g}+\tfrac{3}{2} f_i g_j(\partial_i\partial_j g_k)\partial_k \boldsymbol{f}+\tfrac{25}{32} f_i f_j(\partial_i f_k)(\partial_k f_l)\partial_j\partial_l \boldsymbol{g}+\tfrac{25}{32} f_i f_j(\partial_i f_k)(\partial_j\partial_k g_l)\partial_l \boldsymbol{f}\\
&+\tfrac{1}{256} f_i f_j(\partial_i f_k)(\partial_j f_l)\partial_k\partial_l \boldsymbol{g}+\tfrac{3}{16} f_i f_j f_k(\partial_i\partial_j f_l)\partial_k\partial_l \boldsymbol{g}+\tfrac{1}{64} f_i f_j(\partial_i\partial_j g_k)(\partial_k f_l)\partial_l \boldsymbol{f}+\tfrac{1}{64} f_i f_j f_k(\partial_j\partial_k g_l)\partial_i\partial_l \boldsymbol{f}\\
&+5 g_i(\partial_i f_j)(\partial_j g_k)\partial_k \boldsymbol{f}+\tfrac{5}{2} g_i(\partial_i g_j)(\partial_j f_k)\partial_k \boldsymbol{f}+\tfrac{1}{2} f_i(\partial_i g_j)(\partial_j g_k)\partial_k \boldsymbol{f}+\tfrac{81}{32} f_i(\partial_i f_j)(\partial_j f_k)(\partial_k g_l)\partial_l \boldsymbol{f}\\
&+\tfrac{161}{128} f_i(\partial_i f_j)(\partial_j g_k)(\partial_k f_l)\partial_l \boldsymbol{f}+\tfrac{1}{128} f_i f_j(\partial_i f_k)(\partial_k g_l)\partial_l\partial_j \boldsymbol{f}+\tfrac{3}{8} f_i f_j(\partial_i g_k)(\partial_j\partial_k f_l)\partial_l \boldsymbol{f}+\tfrac{1}{32} f_i f_j(\partial_i f_k)(\partial_j g_l)\partial_k\partial_l \boldsymbol{f}\\
&+\tfrac{3}{16} f_i f_j f_k(\partial_i g_l)\partial_j\partial_k\partial_l \boldsymbol{f}+\tfrac{1}{32} f_i(\partial_i g_j)(\partial_j f_k)(\partial_k f_l)\partial_l \boldsymbol{f}+\tfrac{1}{32} f_i f_j(\partial_i g_k)(\partial_k f_l)\partial_j\partial_l \boldsymbol{f}+\tfrac{3}{16} f_i f_j(\partial_i\partial_j f_k)(\partial_k g_l)\partial_l \boldsymbol{f}\\
&+\tfrac{15}{2} g_i g_j(\partial_i\partial_j f_k)\partial_k \boldsymbol{f}+\tfrac{23}{128} f_i g_j(\partial_j f_k)(\partial_k f_l)\partial_l\partial_i \boldsymbol{f}+\tfrac{11}{4} f_i g_j(\partial_j f_k)(\partial_k\partial_i f_l)\partial_l \boldsymbol{f}+\tfrac{243}{32} f_i g_j(\partial_i f_k)(\partial_k\partial_j f_l)\partial_l \boldsymbol{f}\\
&+\tfrac{9}{16} f_i f_j g_k(\partial_k f_l)\partial_i\partial_j\partial_l \boldsymbol{f}+\tfrac{3}{32} f_i g_j(\partial_i f_k)(\partial_j f_l)\partial_k\partial_l \boldsymbol{f}+\tfrac{9}{16} f_i f_j g_k(\partial_i\partial_j\partial_k f_l)\partial_l \boldsymbol{f}+\tfrac{183}{128} f_i g_j(\partial_i\partial_j f_k)(\partial_k f_l)\partial_l \boldsymbol{f}\\
&+\tfrac{219}{128} g_i(\partial_i f_j)(\partial_j f_k)(\partial_k f_l)\partial_l \boldsymbol{f}+\tfrac{3}{128} f_i f_j g_k(\partial_j\partial_k f_l)\partial_i\partial_l \boldsymbol{f}+\tfrac{1}{384} f_i f_j f_k f_l f_m\partial_i\partial_j\partial_k\partial_l\partial_m \boldsymbol{f}\\
&+\tfrac{1}{192} f_i f_j f_k f_l(\partial_i f_m)\partial_k\partial_j\partial_l\partial_m \boldsymbol{f}+\tfrac{5}{384} f_i f_j f_k f_l(\partial_i\partial_j\partial_k\partial_l f_m)\partial_m \boldsymbol{f}+\tfrac{169}{576} f_i f_j f_k(\partial_i f_l)(\partial_l f_m)\partial_j\partial_k\partial_m \boldsymbol{f}\\
&+\tfrac{1}{512} f_i f_j f_k(\partial_i f_l)(\partial_j f_m)\partial_m\partial_l\partial_k \boldsymbol{f}+\tfrac{41}{576} f_i f_j f_k f_l(\partial_i\partial_j f_m)\partial_k\partial_l\partial_m \boldsymbol{f}+\tfrac{19}{64} f_i f_j f_k(\partial_i f_l)(\partial_j\partial_k\partial_l f_m)\partial_m \boldsymbol{f}\\
&+\tfrac{1}{192} f_i f_j f_k(\partial_i\partial_j\partial_k f_l)(\partial_l f_m)\partial_m \boldsymbol{f}+\tfrac{1}{192} f_i f_j f_k f_l(\partial_j\partial_k\partial_l f_m)\partial_i\partial_m \boldsymbol{f}+\tfrac{53}{576} f_i f_j(\partial_i f_k)(\partial_k f_l)(\partial_l f_m)\partial_j\partial_m \boldsymbol{f}\\
&+\tfrac{403}{288} f_i f_j(\partial_i f_k)(\partial_k f_l)(\partial_j\partial_l f_m)\partial_m \boldsymbol{f}+\tfrac{23}{32} f_i f_j(\partial_i f_k)(\partial_j\partial_k f_l)(\partial_l f_m)\partial_m \boldsymbol{f}+\tfrac{113}{2304} f_i f_j(\partial_i f_k)(\partial_j f_l)(\partial_k f_m)\partial_l\partial_m \boldsymbol{f}\\
&+\tfrac{985}{512} f_i f_j(\partial_i f_k)(\partial_j f_l)(\partial_k\partial_l f_m)\partial_m \boldsymbol{f}+\tfrac{7}{576} f_i f_j(\partial_i\partial_j f_k)(\partial_k f_l)(\partial_l f_m)\partial_m \boldsymbol{f}+\tfrac{7}{576} f_i f_j f_k(\partial_k\partial_j f_l)(\partial_l f_m)\partial_i\partial_m \boldsymbol{f}\\
&+\tfrac{41}{288} f_i f_j f_k(\partial_j\partial_k f_l)(\partial_i\partial_l f_m)\partial_m \boldsymbol{f}+\tfrac{1}{64} f_i f_j f_k(\partial_i f_l)(\partial_k\partial_l f_m)(\partial_j\partial_m \boldsymbol{f})+\tfrac{7}{576} f_i f_j f_k(\partial_i f_l)(\partial_j\partial_k f_m)(\partial_l\partial_m \boldsymbol{f})\\
&+\tfrac{247}{288} f_i(\partial_i f_j)(\partial_j f_k)(\partial_k f_l)(\partial_l f_m)\partial_m \boldsymbol{f}. \qquad \text{(B1)}
\end{aligned}
$$

APPENDIX C: DERIVATION OF THE $\mathcal{O}(v^6)$ EFFECTIVE LAGRANGIAN

Let us outline the derivation of the Lagrangian for the velocity-dependent force Eq. (B1). The general idea is to list all possible tensor structures with the total number of spatial derivatives equal 4, the total power of the velocity equal $2n$, the total power of the $\boldsymbol{f}$ field equal $2m$, and the total power of the $\boldsymbol{g}$ field equal $3-m-n$, with $n=0,\ 1$, $m=1,\ 2,\ 3$, $m+n\leqslant 3$. A large number of the allowed tensor structures is significantly reduced by eliminating the terms incompatible with the known one-dimensional expression. The Lagrangian is taken as the linear combination of these structures with arbitrary coefficients, which are then determined by comparing the corresponding Euler-Lagrange equation to $\dot{\boldsymbol{v}}^{(6)}+\mathcal{F}^{(6)}_{\rm eff}=0$. This can be done for all the terms in Eq. (B1) except the first one,

$$\tfrac{5}{2} v_i v_j v_k v_l(\partial_i\partial_j\partial_k\partial_l f_m)\partial_m \boldsymbol{f}, \qquad \text{(C1)}$$

which includes the fourth power of the velocity. The relevant structure in the Lagrangian is of the form

$$\tfrac{5}{12} v_i v_j v_k v_l[2(\partial_i\partial_j\partial_k \boldsymbol{f})\partial_l \boldsymbol{f}-(\partial_i\partial_j \boldsymbol{f})\partial_k\partial_l \boldsymbol{f}]. \qquad \text{(C2)}$$

It gives the following contribution to the Euler-Lagrange equation:

$$
\begin{aligned}
&-(v_l\partial_l)^2\big\{\tfrac{5}{3} v_i v_j\big[(\partial_i\partial_j f_k)\boldsymbol{\partial} f_k-(\partial_i \boldsymbol{\partial} f_k)\partial_j f_k\big]\big\}\\
&+\tfrac{5}{2} v_i v_j v_k v_l(\partial_i\partial_j\partial_k\partial_l f_m)\partial_m \boldsymbol{f}+\ldots=0, \qquad \text{(C3)}
\end{aligned}
$$

where the second term exactly reproduces Eq. (C1) and the ellipsis stands for the terms which, after the use of the leading-order equation of motion, include at most the second power of the velocity. These terms can be subtracted from the rest of Eq. (B1) and the part of the Lagrangian Eq. (18) corresponding to the resulting expression can be obtained as described in the beginning of this section. The first term in Eq. (C3) cannot be accommodated in this way. However, since for the slow variables $(v_l\partial_l)^2=d^2/dt^2$, this is the second-order time

derivative which can be absorbed into the acceleration term in the equation of motion by the coordinate transformation

$$\dot{\boldsymbol{v}} + \frac{d^2}{dt^2}\left\{\frac{5}{3}v_i v_j[(\partial_i\partial_j f_k)\boldsymbol{\partial} f_k - (\partial_i \boldsymbol{\partial} f_k)\partial_j f_k]\right\} \to \dot{\boldsymbol{v}}', \quad \text{(C4)}$$

where $\boldsymbol{v}' = \dot{\boldsymbol{r}}'$ and $\boldsymbol{r}'$ is given by Eq. (17). Then we need to express the effective Lagrangian in terms of the new variable. Since the correction term in Eq. (17) is $\mathcal{O}(v^4)$, to get the $\mathcal{O}(v^6)$ approximation the coordinate transformation should be taken into account in the leading $\mathcal{O}(v^2)$ part of the effective Lagrangian only. This is done by substituting

$$\boldsymbol{r} = \boldsymbol{r}' - \tfrac{5}{3}v_i' v_j'[(\partial_i\partial_j f_k(\boldsymbol{r}'))\boldsymbol{\partial} f_k(\boldsymbol{r}') - (\partial_i \boldsymbol{\partial} f_k(\boldsymbol{r}'))\partial_j f_k(\boldsymbol{r}')] \quad \text{(C5)}$$

into Eq. (11) and expanding the resulting expression in Taylor series about $\boldsymbol{r}'$, which generates an additional next-to-next-to-leading contribution to Eq. (18). Note that in Eq. (C5) we have replaced $\boldsymbol{r}$ with $\boldsymbol{r}'$ in the correction term, which is valid through $\mathcal{O}(v^6)$.

[1] P. L. Kapitza, Dynamic stability of a pendulum when its point of suspension vibrates, Zh. Eksp. Teor. Fiz. **21**, 588 (1951).

[2] F. C. Moon and G.-X. Li, Fractal basin boundaries and homoclinic orbits for periodic motion in a two-well potential, Phys. Rev. Lett. **55**, 1439 (1985).

[3] N. Friedman, A. Kaplan, D. Carasso, and N. Davidson, Observation of chaotic and regular dynamics in atom-optics billiards, Phys. Rev. Lett. **86**, 1518 (2001).

[4] R. Blatt and D. Wineland, Entangled states of trapped atomic ions, Nature (London) **453**, 1008 (2008).

[5] C. Monroe, W. C. Campbell, L.-M. Duan, Z.-X. Gong, A. V. Gorshkov, P. W. Hess, R. Islam, K. Kim, N. M. Linke, G. Pagano, P. Richerme, C. Senko, and N. Y. Yao, Programmable quantum simulations of spin systems with trapped ions, Rev. Mod. Phys. **93**, 025001 (2021).

[6] T. Oka and S. Kitamura, Floquet engineering of quantum materials, Annu. Rev. Condens. Matter Phys. **10**, 387 (2019).

[7] K. Wintersperger, C. Braun, F. N. Ünal, A. Eckardt, M. D. Liberto, N. Goldman, I. Bloch, and M. Aidelsburger, Realization of an anomalous Floquet topological system with ultracold atoms, Nat. Phys. **16**, 10, 1058 (2020).

[8] W. Paul, Electromagnetic traps for charged and neutral particles, Rev. Mod. Phys. **62**, 531 (1990).

[9] E. A. Cornell, C. Monroe, and C. E. Wieman, Multiply loaded, ac magnetic trap for neutral atoms, Phys. Rev. Lett. **67**, 2439 (1991).

[10] J. Jiang, E. Bernhart, M. Röhrle, J. Benary, M. Beck, C. Baals, and H. Ott, Kapitza trap for ultracold atoms, Phys. Rev. Lett. **131**, 033401 (2023).

[11] A. Fidlin, On asymptotic properties of systems with strong and very strong high-frequency excitation, J. Sound Vib. **235**, 219 (2000).

[12] S. Rahav, I. Gilary, and S. Fishman, Time independent description of rapidly oscillating potentials, Phys. Rev. Lett. **91**, 110404 (2003).

[13] S. Rahav, I. Gilary, and S. Fishman, Effective Hamiltonians for periodically driven systems, Phys. Rev. A **68**, 013820 (2003).

[14] M. Maggia, S. A. Eisa, and H. E. Taha, On higher-order averaging of time-periodic systems: reconciliation of two averaging techniques, Nonlinear Dyn. **99**, 813 (2020).

[15] I. I. Blekhman and V. S. Sorokin, Effects produced by oscillations applied to nonlinear dynamic systems: A general approach and examples, Nonlinear Dyn. **83**, 2125 (2016).

[16] E. Kremer, Slow motions in systems with fast modulated excitation, J. Sound Vib. **383**, 295 (2016).

[17] J. Venkatraman, X. Xiao, R. G. Cortiñas, A. Eickbusch, and M. H. Devoret, Static effective Hamiltonian of a rapidly driven nonlinear system, Phys. Rev. Lett. **129**, 100601 (2022).

[18] J. J. Thomsen and K. L. Ebbehøj, Strong nonlinearity and external high-frequency forcing for controlling effective mechanical stiffness: Theory and experiment, Nonlinear Dyn. **111**, 6985 (2023).

[19] M. Beneke, M. König, and M. Link, The inverted pendulum as a classical analog of the EFT paradigm, Phys. Scr. **99**, 065240 (2024).

[20] P. K. Sahoo and S. Chatterjee, Effects and applications of non-resonant high-frequency excitation on nonlinear systems: A literature review, Nonlinear Dyn. **113**, 7553 (2025).

[21] A. A. Penin and A. Su, Effective theory of classical and quantum particle dynamics in rapidly oscillating fields, Phys. Rev. Lett. **132**, 051601 (2024).

[22] A. Besharat and A. A. Penin, Dynamical confinement and magnetic traps for charges and spins, Phys. Rev. A **113**, 023107 (2026).

[23] N. M. Krylov and N. N. Bogoliubov, *Introduction to Non-Linear Mechanics*, Annals of Mathematics Studies (Princeton University Press, Princeton, NJ, 1949).

[24] N. N. Bogoliubov and Y. A. Mitropolski, *Asymptotic Methods in the Theory of Non-Linear Oscillations* (Gordon and Breach, New York, 1961).

[25] A. H. Nayfeh, *Perturbation Methods* (John Wiley & Sons, New York, 2008).

[26] I. I. Blekhman, *Vibrational Mechanics: Nonlinear Dynamic Effects, General Approach, Applications* (World Scientific, Singapore, 2000).

[27] A. Fidlin, *Nonlinear Oscillations in Mechanical Engineering* (Springer, Berlin, 2010).

[28] J. J. Thomsen, *Vibrations and Stability: Advanced Theory, Analysis, and Tools* (Springer, Cham, 2021).

[29] See Supplemental Material at http://link.aps.org/supplemental/10.1103/46tw-51sh for the computer code for Eqs. (18), (19), (B1), and for the dimensional reduction of Eqs. (18), (19) to Eqs. (21), (22).

[30] B. V. Chirikov, A universal instability of many-dimensional oscillator systems, Phys. Rep. **52**, 263 (1979).

[31] A. Ugulava, L. Chotorlishvili, and K. Nickoladze, Overlapping of nonlinear resonances and the problem of quantum chaos, Phys. Rev. E **68**, 026216 (2003).

[32] A. Ugulava, L. Chotorlishvili, and K. Nickoladze, Quantum-mechanical research on nonlinear resonance and the problem of quantum chaos, Phys. Rev. E **70**, 026219 (2004).

[33] Y. Wang, Z. Zhu, Y. Zhang, and L. Huang, Metastable states and energy flow pathway in square graphene resonators, Phys. Rev. E **97**, 012143 (2018).

[34] R. Plestid and D. H. J. O'Dell, Balancing long-range interactions and quantum pressure: Solitons in the Hamiltonian mean-field model, Phys. Rev. E **100**, 022216 (2019).

[35] P. Sarkar, S. Paul, and D. S. Ray, Subharmonics and superharmonics of the weak field in a driven two-level quantum system: Vibrational resonance enhancement, Phys. Rev. E **104**, 014202 (2021).

[36] Z. Luo, Y. Liu, Y. Li, J. Batle, and B. A. Malomed, Stability limits for modes held in alternating trapping-expulsive potentials, Phys. Rev. E **106**, 014201 (2022).

[37] M. Wanic, Z. Toklikishvili, S. K. Mishra, M. Trybus, and L. Chotorlishvili, Magnetoelectric fractals, magnetoelectric parametric resonance and Hopf bifurcation, Physica D **467**, 134257 (2024).

[38] L. Deng, C. Fang, H. Yu, Y. Wang, Z. Zhu, W. Fu, S. Flach, and L. Huang, Impact of on-site potentials on q breathers in nonlinear chains, Phys. Rev. E **112**, 044202 (2025).

[39] I. Kovacic, R. Rand, and S. Mohamed Sah, Mathieu's equation and its generalizations: Overview of stability charts and their features, Appl. Mech. Rev. **70**, 020802 (2018).

[40] J. Desai and A. Marathe, Combined homotopy and Galerkin stability analysis of Mathieu-like equations, Int. J. Appl. Comput. Math **9**, 4 (2023).

[41] F. M. Arscott, *Periodic Differential Equations: An Introduction to Mathieu, Lamé and Allied Functions* (Pergamon Press, Oxford, 1964).

[42] E. Ince, IV.—Researches into the characteristic numbers of the Mathieu equation, Proc. R. Soc. Edinb. **46**, 20 (1927).

[43] H. W. Broer, I. Hoveijn, M. van Noort, C. Simö, and G. Vegter, The parametrically forced pendulum: A case study in 1 1/2 degree of freedom, J. Dyn. Diff. Equat. **16**, 897 (2004).

[44] D. E. Pritchard, Cooling neutral atoms in a magnetic trap for precision spectroscopy, Phys. Rev. Lett. **51**, 1336 (1983).

[45] W. Petrich, M. H. Anderson, J. R. Ensher, and E. A. Cornell, Stable, tightly confining magnetic trap for evaporative cooling of neutral atoms, Phys. Rev. Lett. **74**, 3352 (1995).

[46] K. B. Davis, M. -O. Mewes, M. R. Andrews, N. J. van Druten, D. S. Durfee, D. M. Kurn, and W. Ketterle, Bose-Einstein condensation in a gas of sodium atoms, Phys. Rev. Lett. **75**, 3969 (1995).

[47] J. Walz, S. B. Ross, C. Zimmermann, L. Ricci, M. Prevedelli, and T. W. Hänsch, Combined trap with the potential for antihydrogen production, Phys. Rev. Lett. **75**, 3257 (1995).

[48] G. B. Andresen, M. D. Ashkezari, M. Baquero-Ruiz, W. Bertsche, P. D. Bowe, E. Butler, C. L. Cesar, S. Chapman, M. Charlton, A. Deller, S. Eriksson, J. Fajans, T. Friesen, M. C. Fujiwara, D. R. Gill, A. Gutierrez, J. S. Hangst, W. N. Hardy, M. E. Hayden, A. J. Humphries, *et al.*, Trapped antihydrogen, Nature (London) **468**, 673 (2010).